Malaysian Journal of Chemistry, 2026, Vol. 28(2), 224-243

An Ultra-Low Interfacial Tension Rhamnolipid Biosurfactant from *Pseudomonas* sp. NR.22 for Petroleum Hydrocarbon Remediation

Fauziah Marpani, Muhammad Syafiq Abu Hassan and Nik Raikhan Nik Him*
Faculty of Chemical Engineering, Universiti Teknologi MARA, 40450 Shah Alam, Selangor Darul Ehsan, Malaysia
*Corresponding author (email: raikhan7952@uitm.edu.my)

The application of ultra-low interfacial tension (IFT) surfactants from chemically modified surfactants is common in the oil and gas field. Chemically modified surfactants, unfortunately, come with various limitations that require a reconsideration. In this research, a bacterial ultra-low interfacial tension (IFT) Rhamnolipid-biosurfactant, NR-Rhamno, produced by *Pseudomonas aeruginosa* NR.22 is introduced as a potential surfactant for the bioremediation of petroleum-based contaminants. The production was conducted using phosphate-limited proteose peptone-glucose-ammonium salt (PPAS) and two modified media containing 1.0% (v/v) diesel and kerosene, respectively. NR-Rhamno was characterized using biochemical and physico-chemical tests, which includes Fourier-transform Infrared Spectroscopy (FTIR), Nuclear Magnetic Resonance (NMR), and Thermogravimetric Analysis (TGA). Foaming (41.13 ± 0.21%) indicated that NR-Rhamno is potentially suitable for the diesel and kerosene remediation. Ultra-low IFT of 0.004 mN/m was obtained after 90 min of contact time. NR-Rhamno was confirmed as a type of glycolipid, with two types of Rhamnose components. The molecules are connected to one or/and two molecules of hydroxy acid(s), containing glycosyl head groups with 2 Rhamnose moieties on the Rhamnoses; and having 2 fatty acid tails (both are β-hydroxy-fatty acids) with $RhaRha_{C10C10}$ components. The presented results indicate the possible application of NR-Rhamno in oil and gas technology and related EOR enhancement in future.

Keywords: Rhamnolipid biosurfactant, ultra-low interfacial tension, glycolipid characterization, diesel and kerosene biodegradation, microbial enhanced oil recovery

Received: September 2025; Accepted: January 2026

Alternative surfactants are needed to secure less invasive and environmentally friendly options of oil and gas related treatments on top of the current inadequate chemical surfactants. Biosurfactants produced by microbes such as *Pseudomonas*, *Bacillus*, and *Starmerella* have shown strong surface-activity, low toxicity, and high biodegradability, making them attractive alternatives to synthetic surfactants in petroleum hydrocarbon remediation and enhanced oil recovery (EOR) [1]. This alternative specifically refers to enhanced oil recovery and oil/water separation that come with lots of challenges. Optimizing these challenges will require abundance of research and compatible data to take control over the current treatments. The current surfactants are mostly unstable under the oil and gas harsh conditions, causing unwanted reactions and potential environmentally issues, toxicity effects, as well as the excessive absorption into the earth's soil. Importantly, many biosurfactants maintain their functionality under harsh reservoir-like conditions (e.g. high salinity, elevated temperatures, and broad pH range), which often degrade or deactivate conventional chemical surfactants used in oil and gas operations [2]. Recent studies have also reported that some biosurfactants not only lower interfacial tension (IFT) to values comparable with or better than synthetic surfactants, but also possess favorable foaming, emulsification, and wettability-alteration properties essential for delaying emulsified crude separation and improving oil displacement efficiency [3]. In as much as chemical surfactants are non-biodegradable, we need to work hard to bring biodegradable materials as reliable surfactants by introducing few potentials readily available at research level.

Potent surface-active compounds are commonly a product of/from a variety of microbial pathways. It has been adapted through the ability of bacterial cells, fungus or actinomycetes to produce them in large scale and were identified as an alternative to batched production of various surfactants from non-microbial sources. Biosurfactants have been reported to have a significant variation of chemical properties and varieties of molecular size [4]. Through many research, biosurfactants have been reported to have low molecular weight of their glycolipid building blocks [4, 5, 6, 7], while their polyanionic heteropolysaccharides were recorded to carry high molecular weight. This is either in the covalent bond

hydrophobic chains or in the complex molecules, the polysaccharides and proteins. The generated biosurfactants will rely substantially to the nutritional factors given or taken by the producers (selected microorganisms). The enormous functions of biosurfactants have driven this product as one of the prominent materials in a lot of applications, such as waste management, health product [8], food industries [9], regulation of environmental control [10], pollution, and contamination [11], as well as in oil and gas related industries [12]. Biosurfactants can be produced by many types of microorganisms, such as *Pseudomonas* species and Gram-negative strains [13]. They have many advantages as compared to the chemically synthesized biosurfactants, such as higher rate of biodegradability; this is because they are conveniently degraded by other microorganisms [14].

Biosurfactants have been proven to demonstrate lower toxicity compared to the chemically acquired surfactants. It was indicated to promote high EC50, which is a tool used to test the effective concentration in reducing the sample population into half (or 50% of the test population). This test is done using a standard concentration [15], in contrast with values carried out in synthetic dispersants. Apart from that, the availability of the raw materials is abundant, thus large scale manufacturing of biosurfactants can be initiated at lower costs and management issues [16].

Unlike the chemical surfactants, most biosurfactants have demonstrated very strong physical properties and are not impacted by chemical and physical elements of the environment, including the ionic strength tolerances [17]. This is particularly important for a successful reaction with polar and non-polar molecules. Biosurfactants have been extensively used in the remediation of water and soil, as well as in the main stages of the oil production chain, such as extraction, transportation, and storage [18–20]. Approximately 2/3 of the crude oil is still in the reservoir after the primary and secondary oil conventional oil recovery due to interfacial tension (IFT) and high viscosity of the crude oil [21]. To enhance the value of residual oil recovery, numerous steps have been adopted in the oil and gas technology physically and chemically. The use of microbial biosurfactants to enhance oil recovery (EOR) has proven to be a better alternative [22]. Biosurfactants from microbes are amphiphilic, with discrete hydrophobic and hydrophilic groups which can provide optimal interfacial properties. Microbes create biosurfactants during their stationary growth phase to help them with substrate bioavailability, metal binding, adherence, and de-adhesion to surfaces, quorum sensing, and pathogenicity [23].

The properties and structural characterization of the NR-Rhamno biosurfactant, which include FTIR, TGA, NMR, and interfacial tension, were laid out. The characterization of the bacteria isolated from a contaminated lake was accomplished using screening methods for biosurfactant production, followed by species identification using specific agar media. Extraction and structural characterization using different analytical techniques were performed accordingly too.

EXPERIMENTAL

Chemicals and Materials

Bacteriological peptone (ultrapure, protein = Nx6.38 ≥ 76.5%), ammonium phosphate monobasic (≥ 98%), sodium chloride (NaCl), calcium chloride (CaCl) (granular, ≤ 7.0 mm, ≥ 93.0%), peptone solution, and glucose were obtained from Sigma-Aldrich (St Louis, MO, USA). Glycerol, nutrient agar nutrient broth, and yeast extract (granulated) were used as supplied from Merck (Darmstadt, Germany). Potassium dihydrogen phosphate (KH_2PO_4, reagent grade, 99%), sodium hydroxide, and *Pseudomonas* agar were purchased from Vetec and Fluka (Darmstadt, Germany). Kerosene with the density of 0.8 g/ml at 25°C was obtained from Sigma-Aldrich (St Louis, MO, USA) and used directly as one of the carbon sources. Diesel was supplied by a local mechanical department with properties listed as density of 820 kg/m^3, lower heating value of 42.67 MJ/kg, viscosity of 2.92 cSt, and final boiling point of 368.2˚C. Other elements of the diesel were recorded as 86% (w/w) Carbon, 12.947% (w/w) Hydrogen and 1% (w/w) Sulfur.

Preparation of Cell Suspension and Laccase Assay

Pseudomonas aeruginosa NR.22 (Ps.NR.22), a Gram negative rod-shaped bacterium, was first isolated from a contaminated lake in Seksyen 14, Shah Alam, Selangor, Malaysia (coordinate: 3˚04'04.3"N 101˚31'01.9"E), as discussed in our previous work [24] (Figure S1). Laccase assay was carried out by using a modified method from Niku-Paavola et al. [25] and the study of Ps.NR.22's ability to grow in diesel and kerosene was conducted according to Nik Raikhan and Khairul Izwan [26]. One Unit Activity of Laccase was determined as the amount required for a transformation of 1 µmol of substrate per minute.

Production of NR-Rhamno

Pseudomonas aeruginosa NR.22 was initially cultured in a nutrient broth containing 1.0 g/L D(+)-glucose, 15 g/L peptone, 6.0 g/L sodium chloride, and 3.0 g/L yeast extract for 24 hours to obtain a fresh stationary-phase culture [27]. A 1% (v/v) inoculum of 5.0×10^6 cells/mL was transferred into 100 mL of sterile Kay's Minimal Medium composing of 0.3 g of $NH_4H_2PO_4$, 0.2 g of K_2HPO_4, 0.2 g of glucose, 0.5 mg of $FeSO_4$, and 0.1 g of $MgSO_4 \cdot 7H_2O$ [28]. Fermentation was conducted for 24 hours at 37°C. Subsequently, 2.0 mL of this 24-hour culture was inoculated into 200 mL of phosphate-limited proteose peptone-glucose-ammonium salt (PPAS) medium containing 1.0 g of NH_4Cl, 1.5 g of KCl, 19.0 g of Tris-HCl, 5.0 g of glucose, 1.0 g of

proteose peptone, and 0.4 g of $MgSO_4 \cdot 7H_2O$ (pH 7.2). To evaluate the effect of hydrocarbon carbon source, the glucose component (5.0 g) was replaced with 1% (v/v) diesel or kerosene. The inoculated flasks were incubated in a water-bath shaker at 250 rpm for 60 hours at 37°C to allow biosurfactant production.

Recovery and Purification of NR-Rhamno

After fermentation, the culture broth was centrifuged at 7,000 rpm for 15 minutes to remove bacterial cells. The clear supernatant was acidified to pH 2.0 to precipitate the biosurfactant, following modified extraction conditions (temperature and pH) adapted from Zhang et al. [29]. The precipitate was extracted with a chloroform:methanol mixture (2:1, v/v) and centrifuged at 12,000 rpm for 30 minutes. The organic layer was transferred to a round-bottom flask and evaporated under reduced pressure using a rotary evaporator until a viscous golden residue was obtained. The concentrated product was subsequently freeze-dried following the method described by Burstone [30], yielding the purified NR-Rhamno biosurfactant for further characterization.

Characterization of NR-Rhamno

The NR-Rhamno biosurfactant was purified and analyzed. The infrared (IR) spectra of the NR-Rhamno biosurfactant were obtained using a Nicolet IS-10 FTIR spectrometer to identify the functional groups of the surfactant. The scan was conducted in the range of 4000 to 500 cm^{-1}, with a resolution of 1.0 cm^{-1} [32]. The structure of the NR-Rhamno biosurfactant was then compared with a standard Rhamnolipid marker. NR-Rhamno diluted in distilled water and the solid form were used to compare the peaks and bonds. A pre-determined amount of NR-Rhamno was suspended in a sterilized buffer to produce rhamnolipid biosurfactant solutions for surface tension, emulsification index, foaming, and oil displacement analyses. All the measurements conducted in this work were replicated thrice. Critical micelle concentration (CMC) analysis was performed using 0.1 to 1 × 10^{-6} % of the NR-Rhamno surfactant. The CMC values were determined using surface tension method with a semilog plot of surface tension versus surfactant concentration [29]. The measurement on a ring tensiometer (Krüss-tensiometer K6) was performed using 50 ml of the Ps.NR.22 supernatant solution at 35°C, with a solution of 0.1% (v/v) from 80% active solution of NR-Rhamno [33]. The interfacial tension was determined using a CSC interfacial DuNuoy tensiometer (Fairfax, VA, USA); various concentrations of NR-Rhamno biosurfactants ranging from 100 to 1000 ppm were used and measured against paraffin oil at 35°C and 45°C [34]. The range of chosen temperature was based on industrial need together with the temperature of standard NR-Rhamno production.

The emulsification index (E24) was deliberated using 6.0 ml of kerosene into the aqueous phase (of Ps.NR.22 supernatant) followed by vortexing for 2 min. The emulsion index (E24) was calculated after 24 hours using Equation 1 [32].

The foaming test was conducted by adding 10 ml of the NR-Rhamno supernatant and shaken for 2 minutes. The foaming formation was measured (in height over its total height, in a 10 ml graduated cylinder) and the percentage was calculated by using Equation 2 [30].

Biosurfactant Gravimetric Quantification and Oil-displacement Test

Representative aliquots (100.0 mL) of cell-free culture supernatant were collected and acidified to pH ≈ 2.0 with 6 M HCl to precipitate the biosurfactant. The acidified supernatant was extracted three times with chloroform: methanol (2:1, v/v), using 100 mL of solvent per extraction.

Combined organic layers were dried over anhydrous sodium sulphate, filtered, and evaporated to dryness under reduced pressure (rotary evaporator) to give the crude biosurfactant residue. The residue was placed in a vacuum desiccator (40°C) until a constant weight was attained and weighed using an analytical balance (±0.01 mg). Biosurfactant concentration was calculated as in Equation 3 [34].

All extractions were performed in triplicate and reported as mean ± standard deviation. The mass applied in the oil-displacement test was calculated from the measured concentration and applied volume: $m = C \times V$.

$$E_{24} = \left(\frac{Height\ of\ the\ emulsified\ layer\ (mm)}{Total\ height\ of\ the\ liquid\ column\ (mm)}\right) x\ 100\% \quad (1)$$

$$\text{Foaming formation} = \left(\frac{Height\ of\ foam\ (mm)}{Total\ height\ (mm)}\right) x\ 100\ \% \quad (2)$$

Concentration C ($g.L^{-1}$) = mass of dried residue (g) / volume of supernatant extracted (L) (3)

Oil Displacement Test

A 10 cm diameter Petri dish was filled with 10.0 mL of distilled water and overlaid carefully with 20.0 mL of crude oil to form a continuous oil layer (modified from Pornsunthorntawee et al. [35]). Using a calibrated micropipette, a single aliquot of 50.0 µL (±1 µL) of biosurfactant solution was dispensed centrally onto the oil surface. The experiment was conducted at 27.0°C. The diameter of the clear oil-free zone formed by the biosurfactant was measured in millimeters (mm) using a ruler or digital calliper. Each condition (biosurfactant sample, negative control = distilled water, positive control = 0.1% v/v Triton X-100) was performed in triplicate (n = 3). The whole procedure was video recorded to verify the timing and displacement behavior.

RESULTS AND DISCUSSION

Growth Evaluation of Ps.NR.22 in PPAS, Kerosene, and Diesel and Relation to Laccase Production

Bacterial growth generally follows four distinct phases, namely the lag, exponential, stationary, and decline phases, which reflect cellular adaptation, active biomass accumulation, growth stabilization, and cell death, respectively. In this study, *Pseudomonas aeruginosa* NR.22 exhibited a short lag phase during the initial 0–6 hours, followed by an exponential growth phase between approximately 6 and 18 hours for all tested carbon sources, as reflected by increases in cell dry weight. The stationary phase was right after, indicating stabilization of cell growth resulting from nutrient limitation and metabolic constraints. The selection of kerosene, PPAS, and diesel was done based on their common occurrence in petroleum-based industrial wastes. Among the tested substrates, laccase activity was highest in the kerosene medium, followed by PPAS and diesel. Similar findings were reported by Mojarad et al. [37], where 10% (v/v) kerosene was used as a carbon source and achieved degradation efficiencies of up to 68% by *Enterobacter cloacae* and approximately 49% by *Enterobacter hormaechei* over a 168-hour (7-day) incubation period.

In the PPAS medium, depletion of available phosphate likely restricted macromolecular biosynthesis, thereby limiting further cell division. Similarly, in kerosene- and diesel-supplemented media, reduced bioavailability and slower assimilation of hydrocarbon carbon sources imposed additional metabolic stress, collectively leading to growth arrest. Under these nutrient-limited conditions, cellular metabolism shifted from active biomass production toward maintenance and adaptive responses, characteristic of the stationary phase. The stationary phase is commonly associated with the induction of secondary metabolite synthesis. In the present study, this phase coincided with enhanced production of rhamnolipid biosurfactants, suggesting that NR-Rhamno production is closely linked to the stationary phase, where metabolic energy is redirected from biomass formation toward biosurfactant secretion. *P. aeruginosa* NR.22 grew significantly in PPAS, diesel, and kerosene, with the highest growth observed in kerosene. The optimum cell dry weight (CDW) recorded in kerosene ranged from 4.00 to 4.20 mg/ml, representing more than a 50% increase compared to PPAS, while growth in diesel was moderately higher than PPAS throughout the fermentation period.

Kerosene was therefore identified as a more favorable carbon source for *Pseudomonas aeruginosa* NR.22's growth compared to PPAS and diesel. The enhanced growth observed in the kerosene-containing medium may be attributed to the presence of energy-rich hydrocarbon fractions that support sustained metabolic activity and adaptive responses in hydrocarbon-degrading bacteria [18, 24]. Kerosene consists primarily of aliphatic and low-molecular-weight aromatic hydrocarbons, which are generally more bioavailable than heavier petroleum fractions and can be assimilated more efficiently by *Pseudomonas* species. This enhanced growth was further supported by higher laccase enzyme production throughout 90 hours of cultivation in kerosene-containing medium (Table 1). Laccase activity in kerosene-grown cultures remained consistently higher than that observed in PPAS- and diesel-grown cultures, suggesting that exposure to complex hydrocarbon substrates induces oxidative enzymes involved in substrate transformation and detoxification [33]. The induction of laccase under these conditions is consistent with its reported role in catalyzing the oxidation of aromatic and phenolic compounds, thereby facilitating hydrocarbon breakdown, and reducing substrate toxicity. In contrast, diesel, which contains higher proportions of long-chain and branched hydrocarbons, may impose greater metabolic constraints, resulting in comparatively lower enzyme activity. Similarly, growth and laccase production in PPAS medium were limited by phosphate availability, which is known to restrict enzyme synthesis and secondary metabolic activity under nutrient-stressed conditions. Figure 1 presents the laccase enzyme activity, expressed in enzyme units (U), measured at 6-hour intervals over a 90-hour fermentation period for cultures grown in kerosene, PPAS, and diesel.

According to Syuhadah and Nik Raikhan [36], laccase is an important enzyme involved in the degradation of heavy metals and long-chain hydrocarbons. At the genetic level, bacteria possess the ability to express catabolic genes that regulate the production of specific enzymes, enabling the degradation of high-molecular-weight and structurally complex compounds that are not commonly utilized as carbon sources. This adaptive response is often enhanced when bacteria are exposed to unfamiliar substrates. In the present study, exposure of *P. aeruginosa* NR.22 to kerosene, PPAS, and diesel induced laccase production at varying levels, reflecting differential metabolic responses toward each carbon source.

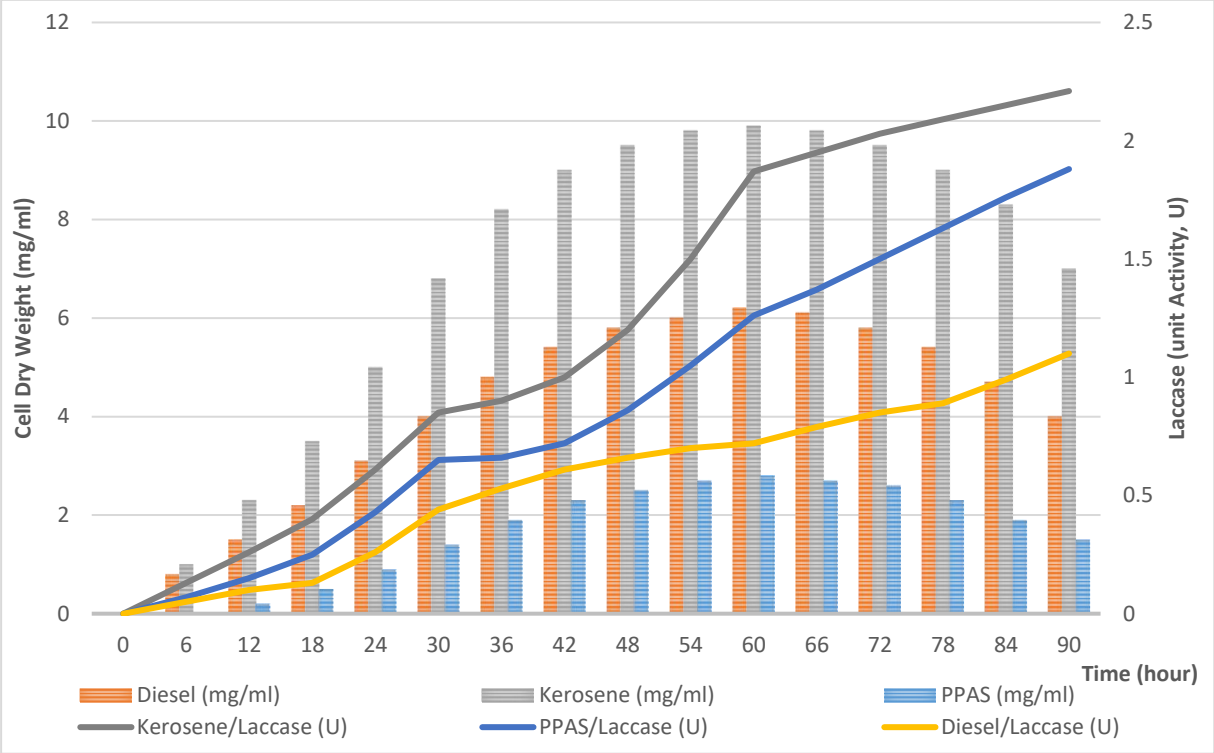

Figure 1. Growth curves and laccase activities by Ps.NR.22 on PPAS, diesel, and kerosene.

Recovery of NR-Rhamno Biosurfactant

Diesel was the least effective carbon source in enhancing NR-Rhamno production, while the PPAS medium provided moderate support for biosurfactant synthesis. The initial yield using PPAS medium was relatively low (0.42 g/L), compared to the industrial-grade or purified rhamnolipids typically reported (1.0–2.0 g/L). To improve productivity, the fermentation medium was modified with 1% (v/v) kerosene and diesel, respectively. The kerosene-supplemented medium recorded the highest NR-Rhamno yield at 1.28 g/L, followed by diesel (0.91 g/L) and PPAS (0.42 g/L).

A comparable improvement was reported for *Bacillus licheniformis*, where modification of the fermentation medium significantly increased lichenysin yield [36]. Similarly, Rodrigues et al. (2006) demonstrated that alternative nutrient media enhanced biosurfactant productivity by *Lactococcus lactis* 53 and *Streptococcus thermophilus* [37]. Moreover, *Pseudomonas aeruginosa* J4 achieved 1.30 g/L (diesel) and 0.709 g/L (kerosene) of rhamnolipid yields under optimized conditions [38] (Table 1).

These results collectively indicate that medium modification and hydrocarbon supplementation effectively enhance biosurfactant productivity. The biosurfactant produced by *Pseudomonas* sp. NR.22 thus represents a viable alternative to synthetic surfactants, emphasizing its potential for petroleum hydrocarbon remediation.

Table 1. Yield of NR-Rhamno in Different Carbon Sources.

Carbon Source / Medium	NR-Rhamno Yield (g/L)	Comparable Literature Yield (g/L)	Reference
PPAS (control)	0.42 ± 0.03	0.5 – 0.8 (*P. aeruginosa*)	[38]
Diesel (1% v/v)	0.91 ± 0.05	1.30 (*P. aeruginosa J4*)	[38]
Kerosene (1% v/v)	1.28 ± 0.04	0.709 (*P. aeruginosa J4*)	[38]
Synthetic medium (reported)	–	1.0 – 2.0 (*industrial grade*)	[36], [37]

Properties of NR-Rhamno Biosurfactant

The biosurfactant production from cells grown in the PPAS medium was excellent and has shown a good correlation with the growth rate (CDW). The low parameters for surface and interfacial tensions and critical micelle concentration of the rhamnolipid-biosurfactant PS indicate its high surface activity [39]. Identifying and monitoring proteins and related components during certain purification processes need a constant homogeneity of the purified fractions. As much as 80% of concentrated semi-purified NR-Rhamno was characterized by FTIR, TGA, and NMR.

FTIR Analysis of Semi-Purified Rhamnolipid

The FTIR spectra of semi-purified NR-Rhamno flakes produced by *Pseudomonas* sp. NR.22 and a reference pure rhamnolipid are presented in Figure 2. The semi-purified sample was selected for FTIR analysis based on its most representative production profile following solvent extraction, precipitation, and crystallization, as described in the previous sections. This sample was therefore considered suitable for qualitative functional group analysis.

FTIR spectroscopy was employed as a qualitative analytical technique to identify characteristic functional groups and to compare the obtained spectrum with that of a reference rhamnolipid. Both spectra exhibited several common absorption bands, indicating that the dominant compound present in the semi-purified sample belongs to the same glycolipid structural class as rhamnolipid (Table 2).

The absorption bands observed at approximately 2924–2943 cm^{-1} and 2854 cm^{-1} are attributed to asymmetric and symmetric stretching vibrations of aliphatic $–CH_3$ and $–CH_2$ groups, corresponding to the hydrocarbon chains of β-hydroxy fatty acids. A prominent absorption band at 1724 cm^{-1} in the pure rhamnolipid spectrum corresponds to ester carbonyl (C=O) stretching, which is a diagnostic feature of rhamnolipid molecules formed by ester linkage between rhamnose and fatty acid moieties.

In the semi-purified NR-Rhamno spectrum, broad absorption bands in the region of 3180–3265 cm^{-1} are associated with O–H stretching vibrations arising from hydroxyl groups of rhamnose units, as well as possible hydrogen bonding due to residual moisture. Absorption bands in the fingerprint region between 1136 and 1045 cm^{-1} correspond to C–O stretching vibrations of ester and alcohol groups, while peaks observed between 909 and 694 cm^{-1} are attributed to C–O–C skeletal stretching and rhamnose ring deformation. These bands are consistent with reported FTIR spectra of rhamnolipids.

Additional minor bands observed at 1628 and 1549 cm^{-1}, as well as weak absorptions in the range of 2240–2099 cm^{-1}, are not characteristic of pure rhamnolipids and are likely attributable to residual organic or proteinaceous impurities resulting from the partial purification process. Such features are commonly reported in semi-purified biosurfactant preparations.

Overall, the close correspondence between the characteristic aliphatic, ester, and carbohydrate-related absorption bands of the semi-purified NR-Rhamno and the reference rhamnolipid supports the presence of rhamnolipid as the dominant component. However, it is acknowledged that FTIR analysis alone provides qualitative evidence and should be interpreted in conjunction with other production and characterization data.

Table 2. FTIR Spectra Comparison of Pure and Semi-Pure NR-Rhamno.

Wavenumber (cm^{-1})	Pure Rhamnolipid (Blue)	Semi-Pure NR-Rhamno (Red)	Functional Group / Assignment	Description
~3265	✓	—	O–H stretching (hydroxyl group)	Broad absorption due to intermolecular hydrogen bonding, typical in rhamnose units.
2924, 2854	✓	2943	C–H stretching ($–CH_2$, $–CH_3$)	Represents aliphatic $–CH_2$ and $–CH_3$ stretching from hydrocarbon chains.
—	3180, 3104	✓	O–H / N–H stretching	Broad peaks associated with hydroxyl and possible amine groups from microbial origin.
1724	✓	—	C=O stretching (ester carbonyl)	Confirms ester linkage between rhamnose and β-hydroxy fatty acid moieties.

Wavenumber (cm^{-1})	Pure Rhamnolipid (Blue)	Semi-Pure NR-Rhamno (Red)	Functional Group / Assignment	Description
—	1628, 1549	✓	C=O stretching (amide/carbonyl)	Indicates carbonyl or amide vibrations, possibly from residual organic compounds.
1574, 1396	✓	—	O–H bending / C–H deformation	Rhamnose ring deformation and alkane bending vibrations.
—	1460, 1402	✓	CH_2 / CH_3 bending	Represents symmetric and asymmetric bending of aliphatic groups.
1122, 1045, 980	✓	1136, 1295	C–O stretching	Ester and alcohol C–O stretching vibrations characteristic of glycolipids.
915, 830, 807, 704, 662, 541	✓	909, 694, 661, 596	C–O–C and ring deformation	Rhamnose ring vibrations and ether (C–O–C) skeletal stretching.
—	2240, 2099	✓	C≡C or C≡N stretching	Possibly due to impurities or unsaturated carbon species present in semi-pure sample.

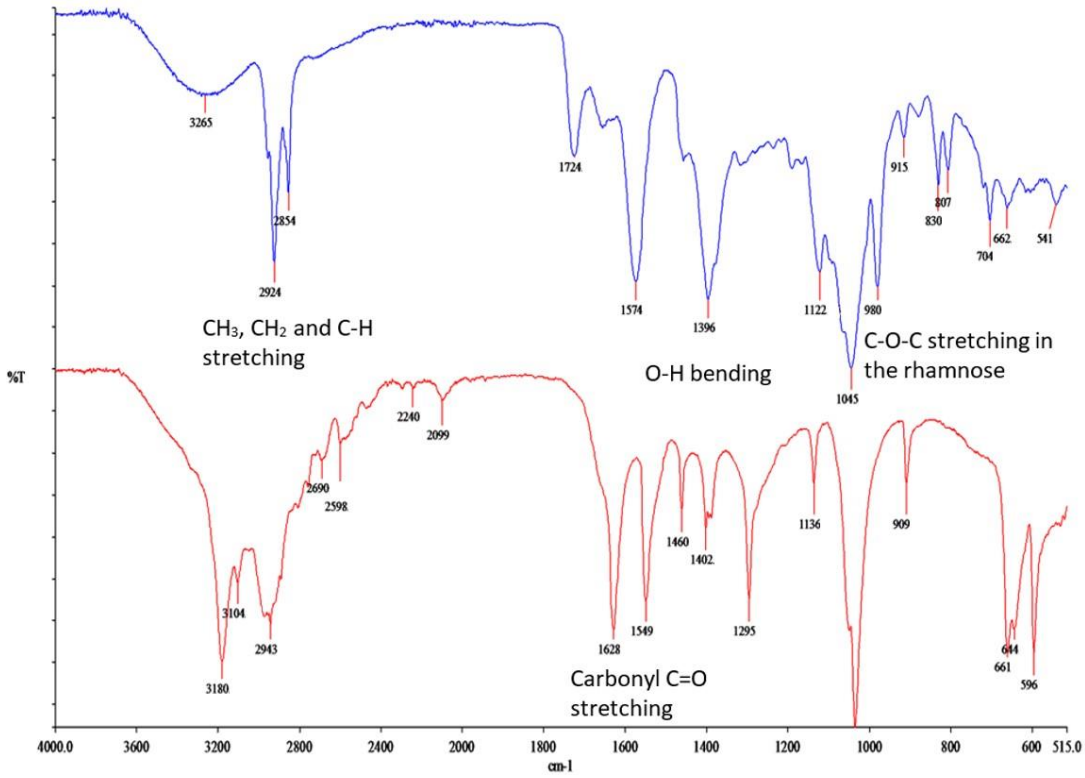

Figure 2. FTIR spectra for solid pure Rhamnolipid (blue) and semi-pure NR-Rhamno (red).

Thermogravimetric Analysis (TGA)

Thermogravimetric analysis (TGA) was conducted to evaluate the thermal stability and decomposition behavior of the semi-purified NR-Rhamno. The TG and corresponding DTG curves are presented in Figure 3(a) and Figure 3(b), respectively.

The TG curve shows an initial minor weight loss below 150°C, which is attributed to the evaporation of physically adsorbed moisture and volatile components. A major weight loss event is observed between approximately 230 and 320°C, indicating the primary thermal degradation of the rhamnolipid structure. This stage is associated with

the decomposition of ester linkages and fatty acid chains, which is characteristic of glycolipid biosurfactants.

The DTG curve exhibits a pronounced peak centerd at approximately 260–280°C, corresponding to the maximum rate of mass loss during the main decomposition stage. This thermal behaviour is consistent with previously reported rhamnolipid degradation profiles. A gradual and continuous mass loss observed at temperatures above 400°C may be attributed to the decomposition of residual carbonaceous matter.

Overall, the TGA results indicate that the semi-purified NR-Rhamno exhibits moderate thermal stability, with the primary degradation occurring above 230°C, supporting its potential applicability in processes requiring thermal resistance within this range.

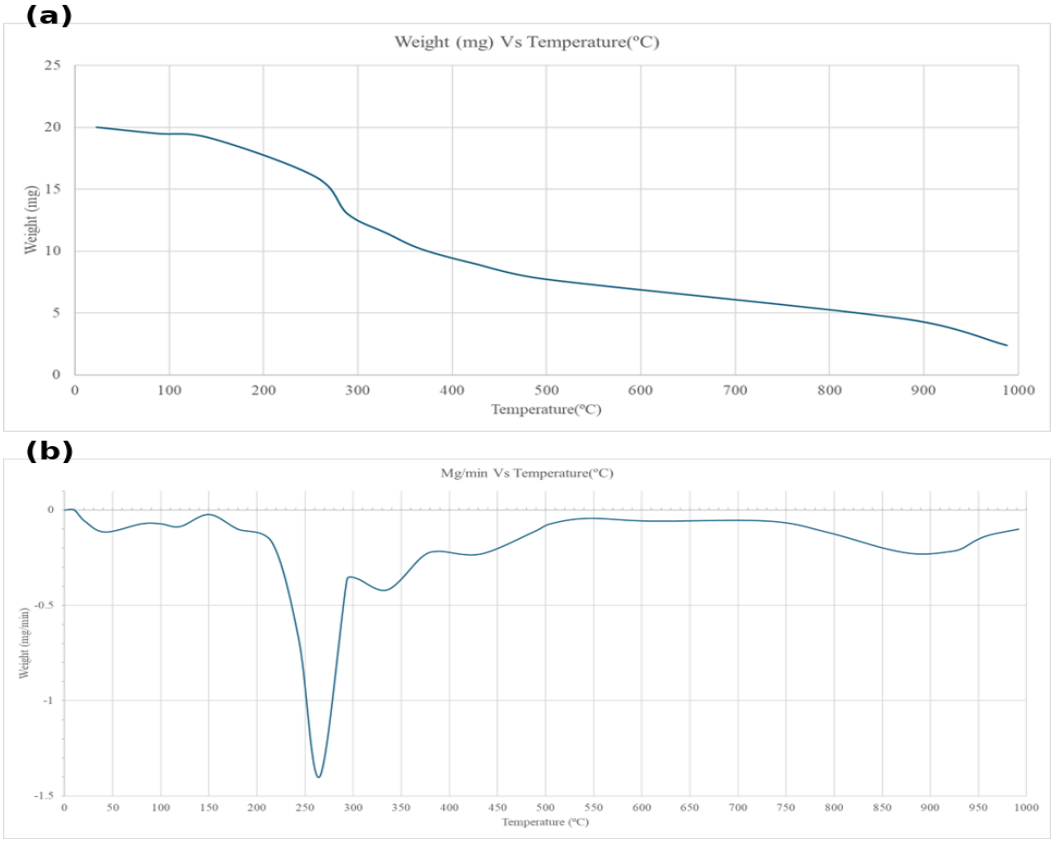

Figure 3. Thermogravimetric analysis (TGA) of semi-purified NR-Rhamno: (a) thermogravimetric (TG) curve showing weight loss as a function of temperature, and (b) derivative thermogravimetric (DTG) curve indicating the rate of weight loss.

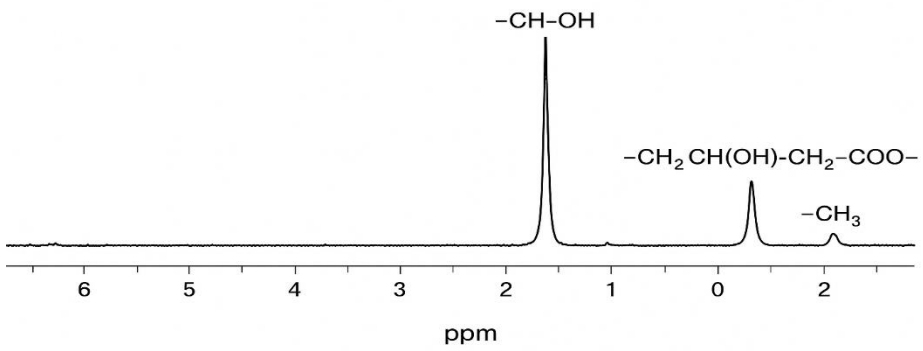

Figure 4. NMR spectrum of NR-Rhamno biosurfactant (400 Mhz, D_2O).

Nuclear Magnetic Resonance (NMR) Study

Both semi-pure and pure rhamnolipids were compared for the basis of the component determination. Figure 4 shows the NMR spectrum of NR-Rhamno with the assignments for a few significant peaks. To further analyze the possible components of the semi-pure NR-Rhamno, ^{1}H shift chemical peaks were identified. Table 3 shows the NMR ^{1}H chemical shifts, assignments, and types of bonds for the semi-pure NR-Rhamno. The semi-pure NR-Rhamno showed singlet and duplet multiplicities with 4 different types of assignments. These details were used to determine the bond types where 2 types of major bonds were identified. At ^{1}H chemical shifts 1.183 and 1.192 ppm, for example, we recorded a doublet arrangement with -CH_3, -CH_3, and the relevant type of bond name for this shift is a Rhamnose moiety. For the ^{1}H chemical shifts of 2.135 and 2.118 ppm, the doublet was again recorded with the assignment of -CH(O)-CH_2COO to represent β-hydroxyfatty acid. The rest of ^{1}H chemical shifts of 3.337, 3.372 and 4.935 ppm recorded 2 different kinds of singlets (-CH-OH and -(CH2)-CH(O-Ra)-CH_2COO). Both represent β-hydroxyfatty acid and 2 Rhamnose moieties. By using the data and information, the possible structure of the semi-pure Rhamnolipid Ps.NR.22 was designed. Figure 5 represents the obtained structure of NR-Rhamno, appeared to be a glycolipid group biosurfactant. NR-Rhamno is structured to be a di-Rhamnolipid, having two Rhamnose congeners that are linked to one or two molecules of hydroxy acid(s). It is comprised of glycosyl head groups with these 2 Rhamnose moieties on the Rhamnose; (-CH_3 and -CH-OH), having 2 fatty acid tails, both are β-hydroxyfatty acids and having $RhaRha_{C10C10}$ components in the structure. These characteristics have significantly confirmed a strong structure of many common Rhamnolipids. Based on this scientific finding, we strongly believe the semi-pure biosurfactant from Ps.NR.22 is a di-Rhamnolipid. Ghadir et al. [44] has classified a rhamnolipid consisting of β-hydroxyl (3-hydroxy) fatty acids bonded to one another by a linkage named O-glycosidic linkage. This linkage was proposed to be a 2-rhamnose sugar molecule.

The study on the structure of rhamnolipid-biosurfactants using NMR chemical shift was first done by Eraqi et al. [45] in 1992, which reported on the structure of the extracellular rhamnolipid (α-L-rhamnopyranosyl-3-hydroxydecanoyl-3-hydroxydecanoate and α-L-rhamnopyranosyl-(1→2)-αL-rhamnopyranosyl-3-hydroxydecanoyl-3-hydroxydecanoate). Both rhamnolipids were isolated from the culture broth of *Pseudomonas aeruginosa* grown under growth-limiting conditions. In 2010, scientists identified the structure of a rhamnolipid from *Pseudomonas aeruginosa* MR01. The extracted biosurfactant has been analyzed to be incorporated by two types of compounds namely, mono- and di-rhamnolipids. The identity of the two structurally distinguished rhamnolipids was confirmed by ^{1}H and ^{13}C nuclear magnetic resonance (NMR) spectroscopy [46]. The finding of the structure of the locally isolated Rhamnolipid NR-Rhamno through the above discussion has added to the number of the relevant new rhamnolipids that can widen the research scope of the Rhamnolipid, especially towards the oil and gas and EOR development.

Table 3. NMR ^{1}H chemical shifts, assignments, and types of bonds for semi-pure NR-Rhamno.

Chemical Number	^{1}H shift chemical shift (ppm)	Multiplicity	Assignment	Type of bond
1	1.182, 1.192	Doublet	-CH_3	Rhamnose moiety
2	2.135, 2.118	Doublet	-CH(O)-CH_2COO	β- hydroxyfatty acid
3	3.337	Singlet	-CH-OH	Rhamnose moiety
4	3.372	Singlet	-(CH_2)-CH(O-Ra)-CH_2COO	β-hydroxyfatty acid
5	4.935	Singlet	-CH-OH	Rhamnose moiety

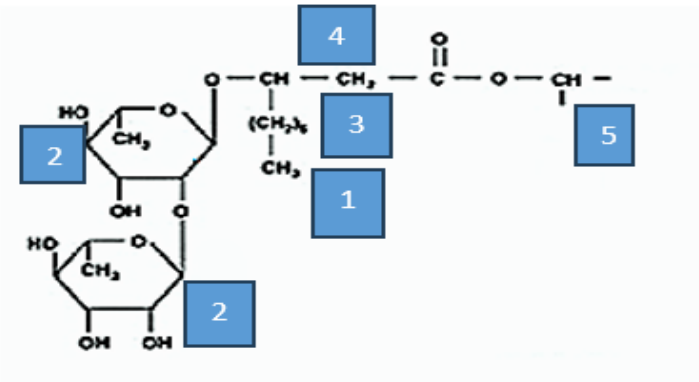

Figure 5. Obtained structure of NR-Rhamno by using ^{1}H NMR.

The production of NR-Rhamno by using 1% (v/v) kerosene was recorded as the most significant (as in qualitative measurement), therefore it was projected as the best production medium for NR-Rhamno. The characteristics of NR-Rhamno were studied through surface tension, emulsification index, and cell micelle concentration. The direct measurement of the interfacial or surface activity of the culture supernatant is the most straightforward test method and very appropriate to confirm a biosurfactant. Surface tension decreased with increasing surfactant concentration until CMC was reached, which means if the concentration of NR-Rhamno was recorded above its CMC, an increase in the NR-Rhamno concentration would not be detected. CMC correlates to the biosurfactant concentration, where surface tension of 2 different concentrations may be recorded the same. This is especially true with certain bacterial species producers. CMC is affected by factors such as pH and ionic strength, as well as the appearance of fatty acids or mono/di-glycerides at interfacial activity.

Figure 6 shows the emulsification index (E24), surface tension, and critical micelle concentration (CMC) of the kerosene-produced NR-Rhamno at various incubation periods versus cell growth. A good biosurfactant is reported to have reduced the surface tension of water from 72 to 35 mN/m but a *Pseudomonas* species was reported to lower water surface tension to 34 mN/m [44]. NR-Rhamno reduced the surface tension from 49 mN/m to 34 mN/m in 54 hours starting from 18 hours to 60 hours of cell incubation (Figure 6B). This is contributed by the thermal degradation of NR-Rhamno at the beginning of the exposure to the temperature before it started to stabilize and reached steady state (Figure 4). Growth evaluation of Ps.NR.22 supports the NR-Rhamno concentrations and the results are established in Figure 6A, as the increase in growth increased the concentration of NR-Rhamno. NR-Rhamno started to be produced at 6 hours and increased constantly until 48 hours of fermentation. The critical micelle concentration (CMC) for NR-Rhamno at 90 hours is shown in Figure 6B with the highest value, recorded at 0.045 mg/l or 45 g/L. Matsufuji et al. [50] produced about 32 g/L of Rhamnolipid by using *Pseudomonas aeruginosa* IFO 3924 in a fed-batch system with 55.3 g/L of ethanol, and expressing excellent CMC. NR-Rhamno has better CMC due to the better cell mass (growth), which relates to the Ps.NR.22 that appeared to be a supreme species. The rhamnolipid's concentration has been concluded as achieving one of the highest final Rhamnolipid ever reported in formal literature. Mulligan [49] has reported that 230 mg/L of rhamnolipid was produced by using high proportions of congeners containing unsaturated fatty acids. While Paulino et al. [52] and Nitschke et al. [53] have reported that rhamnolipid production was achieved as 5 mg/L for di-Rhamnolipids with C_{10} fatty acids and 40 mg/L for mono-rhamnolipids with C_{10} fatty acids, respectively.

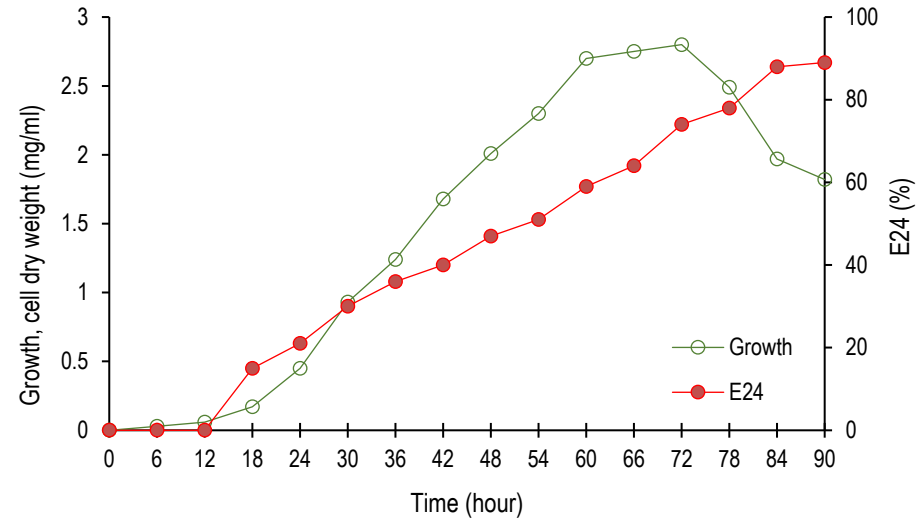

(a)

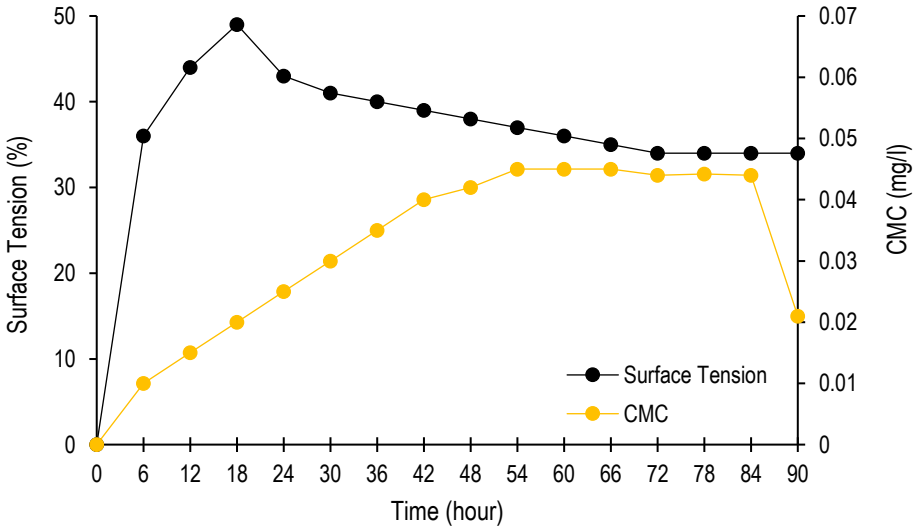

(b)

Figure 6. (a) Emulsification index (E24) and growth; and (b) critical micelle concentration (CMC) and surface tension of the kerosene-produced NR-Rhamno at various incubation periods versus cell growth.

Interfacial Tension (IFT) Analysis of NR-Rhamno

The interfacial tension of NR-Rhamno was evaluated over time with 1.0 ml of 0.1 % (v/v) NR-Rhamno, diluted from 80 % (w/v) NR-Rhamno concentration, at pH 7.1 (at 52˚C) in sea water medium (brine) for 120 minutes of contact time (Figure 7). A sudden decrease of IFT value waa observed at contact time 20 to 30 min of exposure (Figure 7), but it became stable from contact time 30 to 120 min with IFT between 0.03 (30 min) to 0.004 (90-120 min) (Figure 7). NR-Rhamno was observed to achieve ultra-low interfacial tension (IFT) of 0.004 mN/m after 90 minutes, measured by using a spinning drop tension meter test. The ultra-low IFT was stable for 40 min, suggesting high stability of NR-Rhamno towards interfacial interaction even at a very low concentration. Table 4 summarizes the IFT values of rhamnolipid biosurfactants produced from *Pseudomonas* strains from different sources from literature search from the year 2015. As could be observed from reported literature, the IFT value in this study is known to be the lowest so far.

Since ultra-low IFT from fresh bacterial rhamnolipids was almost impossible before, some scientists were reporting on formulating biosurfactant mixtures to achieve ultra-low IFT values against hydrocarbon components [58]. They tested the interfacial activity of biosurfactants from individual strains and with some mixtures of the selected biosurfactants gained/produced from different kinds of strains. It was tested either with or without a synthetic surfactant. The results have been promoted for a multiple regression analysis that showed lipopeptide biosurfactants from various *Bacillus* species having many interfacial activities against toluene, depending on the relative proportions of 3-OH-C14, C15, C16, and C18 in the fatty acid tail. This can be concluded as the fatty acid composition became more heterogeneous in the system to produce lower IFT against toluene. Such a report proved that achieving ultra-low IFT rhamnolipid, or even any biosurfactants, was almost impossible until the IFT of NR-Rhamno proved otherwise. NR-Rhamno can be highlighted as a huge potential in not only oil and gas industry but any related industries that hydrocarbons become its main subjects.

Lots of factors will eventually give effect to the stability of achieved lower IFT and the ability to reach ultra-low values as well. Cell growth conditions, chemical addition, contact time, surfactant interactions, chemical-physical interaction, temperature, salinity, and even thermal stability have been identified as factors. Even at the best optimum growth conditions, microbial life has never been projecting the same ability to produce their metabolites with the same imitated characteristics, including during the production of biosurfactants. This is due to the related mechanism that has always being affected by cell-to-cell communication, as well as the enzymatic activities and microbial self-sustainability to reproduce. Lots of rhamnolipids are produced together with Laccase enzymes. There are always unachieved quality issues whenever biosurfactants are re-produced. Aiming for a re-production with the same quality of biosurfactant would cause the cost to rise. According to Zhao et al. [55], biosurfactants could potentially be replaced or be used in conjunction with synthetic surfactants to provide for more cost-effective subsurface remediation and therefore there is a huge possibility that ultra-low IFT can be achieved. The design of surfactant formulations that are effective in lowering interfacial tension (IFT), which is necessary to mobilize entrapped hydrocarbons, requires information about the surface-active agent (surfactant) and the targeted non-aqueous phase liquids (NAPL). This idea may work but still, deep approach research needs to be done to ensure the maintaining of low-interfacial-tension biosurfactants is achieved continuously and excellently.

Table 4. Interfacial tension values of Rhamnolipidtype biosurfactants from different sources of strain.

Strain type	*Pseudomonas aeruginosa NR.22*	*Pseudomonas aeruginosa DYNA270*	*Pseudomonas stutzeri Rhl*	*Pseudomonas SWP-4*	*Pseudomonas aeruginosa*	*Pseudomonas aeruginosa*	*Pseudomonas aeruginosa DN1*
Source	Contaminated lake	Soil isolate	Oilfield-produced water	Waste cooking oil-contaminated sludge	Wastewater from oil field	No information	Petroleum-contaminated soil
IFT (mN/m)	0.004	0.05	0.169	0.9	1.17	1.2	4.59
Ref.	This study	[52]	[53]	[54]	[56]	[56]	[57]

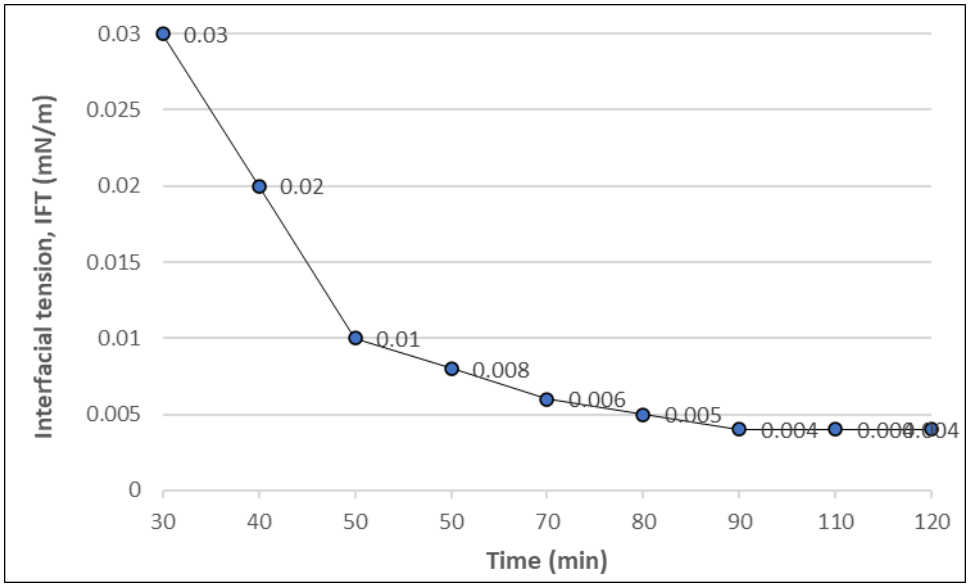

Figure 7. NR-Rhamno at 0.1% (v/v) concentration in Sea Water Medium with IFT values recorded for 120 minutes of contact time.

The performance of the NR-Rhamno biosurfactant from *Pseudomonas aeruginosa* NR.22 demonstrated a remarkable reduction of surface tension from 49 mN m^{-1} to 34 mN m^{-1} at its critical micelle concentration (CMC), indicating efficient molecular packing at the air–water interface. The corresponding interfacial tension (IFT) against diesel reached an ultra-low value of 0.004 mN m^{-1} after 90 min of contact, confirming its strong surface activity and potential in hydrocarbon remediation. In contrast, conventional synthetic surfactants such as sodium dodecyl sulfate (SDS) and Triton X-100 typically achieve surface tensions around 38–40 mN m^{-1} and IFT values not lower than 0.1 mN m^{-1} under comparable conditions [59, 60]. Moreover, the foaming capacity of NR-Rhamno (41.13 ± 0.21%) and its stability at 27–45°C indicate functional robustness superior to most chemical surfactants, which often lose efficiency under elevated temperatures and high salinity environments [61]. The synergistic rhamnose moieties and β-hydroxydecanoic acid (C_{10}) chains contribute to stronger amphiphilic interactions with diesel hydrocarbons, explaining its enhanced dispersion and emulsification performance. These findings highlight that the naturally derived NR-Rhamno achieves comparable or even greater interfacial efficiency than synthetic surfactants, while maintaining biodegradability and lower toxicity, which are advantageous for sustainable oil and gas applications.

Quantitative Oil Displacement Test Findings

Oil displacement test, or oil-spread test, is among the finest qualitative tests for biosurfactant confirmation. Most reports will present clear zones formed by the supernatants (or the targeted biosurfactants) onto a surface of water covered by the chosen oils. Ariech and Guechi [62] reported valuable biosurfactant screening methods, disclosing linear correlations between oil spreading methods and the surface tension. The findings have been compared using different surfactants from different microbial sources and it was concluded as a significant method for biosurfactant detection, as well as for biosurfactant characterization. Lan et al. [56] reported that the diameter of the clear zones where oil is displaced will significantly relate to the concentration of the supernatant used (microbial surfactants), but as this method has not been introduced quantitatively, it often being questioned as not thorough, even though it is among the most popular methods.

In this paper, modifications to the oil displacement test have been applied, where clear zones are reported in quantitative data using percentage over the original oily zones. Table 5 exhibits photos of oil displacement and the percentage of clear zones achieved in the oil displacement test using NR-Rhamno (which was achieved in only 2 seconds). When 0.5 ml (0.1%, v/v) of NR-Rhamno was dropped onto the crude oil at 27°C, a very fast oil separation (clear zones) with recorded maximum diameter of 95 mm was produced in the petri dish. Percentages of clear zones produced were calculated and represented in Table 5; with optimum oily zone clearance recorded between 24% to 95%.

In many scientific studies, crude oil was named the most compelling carbon source to prove the ability of biosurfactant reactivity in displacement. Apart from that, Nik Raikhan and Syuhadah [36] studied the ability of *Pseudomonas aeruginosa* NR22 to produce

a biosurfactant using three impactful concentrations of 4 types of crude oil (2%, 5% and 7%, w/v), and reported the survival of the cells on all three concentrations (in all types of crude oils) with high specific growth rate and overall crude oil degradation stated nearly 97%. Through this study, a biosurfactant was isolated as one of the components in the fermentation products. The biosurfactant was separated and purified for further studies. This consequential finding has proved the biosurfactant as a dominant molecule over any crude oils and it is able to shift molecules of crude oils without any energy demand or physical forces. It can happen very fast and absolutely with clean and clear results quantitively or qualitatively. Isty et al. [63] cultured *Pseudoxanthomonas taiwanensis* on SMSS medium containing crude oil and reported crude oil as the most relative source of carbon in producing a biosurfactant. The effectiveness of the biosurfactant has been proven through a test versus an activity of SDS (sodium dodecyl sulfate) in reducing IFT, as well as using the oil displacement test.

Table 5. Percentage of zones achieved in the oil displacement test using NR-Rhamno recorded in a 2-second recorded video.

Time (second:frame)	Photo	Clear Zones (mm)	Percentage Over Oily Zones (%)
00.09	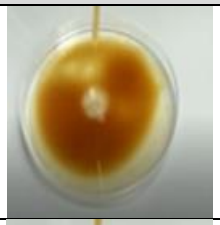	24.00	24%
00.23		42.00	42%
00.43		61.00	61%
01.01	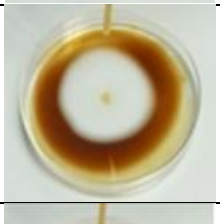	65.00	65%
01.68		87.00	87%
02.00		95.00	95%

As a promising biosurfactant in an oil and gas industry, NR-Rhamno has been the first of its kind to achieve an ultra-low IFT at 0.004 mN/m. According to Syuhadah and Nik Raikhan [39], higher activity was recorded when the ratio of biosurfactant to Asp/Glu-methyl ester remains its similar activity irrespective of the pH change. This condition is not easily achieved because pH of any reaction varies and changes according to conditions. But for NR-Rhamno, both factors were not becoming a challenge. Other biosurfactants that have a very high potential for MEOR were *Pseudoxanthomonas taiwanensis* cultured on SMSS medium [54]. Crude oil was recorded to be the most effective carbon source for biosurfactant production, but there was no report on IFT characteristics. Table 6 presents characteristics of Rhamnolipids in comparison with the readily available chemical surfactants using various researchers' findings.

The comparative evaluation of rhamnolipid biosurfactants against conventional surfactants highlights both opportunities and limitations in petroleum remediation. Rhamnolipids consistently reduce water surface tension to ~25–32 $mN \cdot m^{-1}$ and can achieve ultra-low oil–water interfacial tensions (<1 $mN \cdot m^{-1}$) under saline conditions, rivaling or exceeding the performance of synthetic dispersants, such as dioctyl sodium sulfosuccinate (DOSS) formulations [64, 65]. In contrast, widely used surfactants like sodium dodecyl sulfate (SDS) and Tween-80 show higher equilibrium interfacial tensions (≈3–5 $mN \cdot m^{-1}$ in oil–water systems) and less pronounced sensitivity to ionic strength [66, 67]. A key distinction lies in critical micelle concentration (CMC): rhamnolipids exhibit CMCs in the 10–230 $mg \cdot L^{-1}$ range, significantly lower in molar terms than SDS (≈8–10 mM), suggesting more efficient micelle formation at environmentally relevant concentrations [68]. Beyond physicochemical activity, biodegradability profiles further separate these classes; rhamnolipids are readily degraded in natural environments, while synthetic dispersants raise concerns over persistence and ecotoxicity [69]. Nevertheless, challenges such as production cost, variability in congener mixtures, and scale-up remain barriers to replacing synthetics in large-scale applications. Taken together, the data suggests that while rhamnolipids offer a greener and highly effective alternative, strategic integration with or substitution for commercial surfactants must balance performance, economics, and environmental impact.

Table 6. Chemical Reaction and Structure of Rhamnolipids Versus Commercial Surfactants.

Property (units)	Rhamnolipids (biosurfactant) — typical range	Representative commercial surfactants — typical ranges
Critical micelle concentration (CMC)	~10 – 230 $mg \cdot L^{-1}$ (0.01–0.23 $g \cdot L^{-1}$); depending on congener, purity, ionic strength, and temperature [75]	SDS (anionic): ~2.3 $g \cdot L^{-1}$ (≈8–10 mM) in pure water at 25°C (CMC decreases in presence of salt). Tween-80 (nonionic): ~10–15 $mg \cdot L^{-1}$ (reported as ≈2.5–13 $mg \cdot L^{-1}$ depending on method); DOSS (dioctyl sodium sulfosuccinate): CMC variable in salt water, often lower than SDS (mM range).
Equilibrium surface tension of water (min, $mN \cdot m^{-1}$)	~25–32 $mN \cdot m^{-1}$ at or above CMC for many RL preparations. (Some reports 28–30 $mN \cdot m^{-1}$) [72].	SDS: ~36–37 $mN \cdot m^{-1}$ at/above CMC (depends on purity & ionic strength); Tween-80: lowers to ~30–35 $mN \cdot m^{-1}$ (nonionic behavior); DOSS/Corexit components can produce surface tensions comparable to or lower than synthetic anionics in formulations.
Interfacial tension (oil–water) achievable ($mN \cdot m^{-1}$)	Can reach <1 $mN \cdot m^{-1}$ under optimized conditions (seawater salinity, pressure/temperature, or with co-solutes) — several studies report IFT between crude oil and water below 1 $mN \cdot m^{-1}$ with rhamnolipids [62]	DOSS-containing dispersants (e.g., Corexit) and tailored synthetic dispersants are formulated to rapidly reduce oil–water dynamic IFTs to low values (often sub-$mN \cdot m^{-1}$ transiently for effective dispersion). SDS/Tween alone typically produce higher equilibrium IFTs vs tailored dispersants [75]
Emulsification index (E24, %)	~50–80% for many rhamnolipid preparations (good emulsifiers for hydrocarbons) [72]	Tween-80 and synthetic nonionics: often good emulsifiers (E24 variable ~30–80% depending on oil). DOSS-based formulations are optimized for dispersion rather than long-term emulsion stability [68].
Charge / chemical nature	Anionic glycolipid(s) — monorhamnolipids & dirhamnolipids (rhamnose + β-	SDS: small anionic alkyl sulfate (single defined molecular species). Tween-80: nonionic polyoxyethylene sorbitan monooleate

	hydroxy fatty acid(s)); mixture of congeners with chain lengths/saturation. This mixture influences packing, CMC and IFT [72]	(polymeric/PEG chain). DOSS: anionic sulfosuccinate (amphiphilic small molecule)
Molecular weight (typical)	Mixture: ~350–650 Da depending on congener (mono- vs di-rhamnolipid, fatty acid chain lengths) [72].	SDS ~288 Da; Tween-80 (polydisperse) average Mw ~1310 Da; DOSS ~444 Da (values depend on formulation).
Stability: pH, temperature, salinity	Generally robust: many RLs remain surface-active over broad pH, temperature and salinity ranges; salt (NaCl) often lowers CMC and can improve IFT reduction in seawater — beneficial for marine remediation. [70]	SDS: ionic strength affects micellization; nonionics (Tween): temperature (cloud point) can be limiting; DOSS/dispersants are formulated to act in seawater but may show different dynamic behavior under temperature/salinity extremes.
Biodegradability	Generally, readily biodegradable (but rate depends on purity, congener and matrix); many studies show RLs biodegrade faster than many synthetic surfactants in natural systems [73]	Tween-80: inherently biodegradable in many environments but can sorb to solids; SDS: biodegradable but sometimes slower and subject to environmental persistence/accumulation in certain matrices; DOSS/Corexit components: biodegradability observed but concerns exist regarding persistence/metabolites and ecotoxicity in some ecosystems. [73]
Ecotoxicity / acute toxicity	Low to moderate depending on concentration and purity; RLs often less toxic than some synthetic dispersant formulations in equivalent functional concentrations, but effects are species- and dose-dependent [62].	SDS: marine toxicity at moderate concentrations; Corexit/DOSS: documented acute toxicity in some species (LC50s in tens of $mg \cdot L^{-1}$ for some organisms), concerns over mixtures and metabolites during oil spill responses. [77].

CONCLUSION

The present study successfully demonstrated the production and characterization of an ultra-low interfacial tension (IFT) rhamnolipid biosurfactant, NR-Rhamno, synthesized by *Pseudomonas aeruginosa* NR.22 using proteose peptone-glucose-ammonium salt (PPAS) medium with diesel as an inducer. The biosurfactant reduced surface tension from 49 to 34 mN m^{-1} and achieved an IFT of 0.004 mN m^{-1} against diesel after 90 min, indicating exceptional surface activity. These results are comparable or superior to previously reported rhamnolipids from *Pseudomonas* species, which typically exhibit surface tensions in the range of 30–35 mN m^{-1} and IFT values between 0.01 and 0.05 mN m^{-1} [66, 59].

The NR-Rhamno biosurfactant also exhibited stable foaming activity (41.13 ± 0.21%) and temperature tolerance up to 45°C, consistent with reports by Li et al. [60] and Singh & Van Hamme [61], who observed performance decline of synthetic surfactants under similar conditions. The combination of dual rhamnose head groups and β-hydroxydecanoic acid (C_{10}) tails provides enhanced amphiphilic interaction with diesel hydrocarbons, resulting in efficient dispersion and emulsification. Compared to conventional surfactants such as SDS, Tween 80, and Triton X-100, which generally show IFT values above 0.1 mN m^{-1}, NR-Rhamno offers higher efficiency with the added advantages of biodegradability and low toxicity.

Overall, this study highlights the potential of NR-Rhamno as a sustainable and high-performance alternative for petroleum hydrocarbon remediation and enhanced oil recovery applications. Further optimization of large-scale production and formulation stability could pave the way for industrial implementation in oil and gas processes.

ACKNOWLEDGEMENT

The authors would like to thank the Faculty of Chemical Engineering, Universiti Teknologi MARA for the laboratory, chemical, and technical supports during this research was taking place.

REFERENCES

1. Andrade, A., Mehl, A., Mach, E., Couto, P. and Mansur, C. R. E. (2024) Application of biosurfactants in enhanced oil recovery ex-situ: a review. *Brazilian Journal of Microbiology*, **55(4)**, 3117-3139. doi: 10.1007/s42770-024-01515-7.

2. Patrícia, S. da Silva M., Renata, R. da Silva and Juliana, M. de Luna (2022) Microbial biosurfactants and environmental applications: a narrative review. *Research, Society and Development*, **11(12)**. DOI: https://doi.org/10.33448/rsd-v11i12.34123

3. Purwasena, I. A., Amaniyah, M., Astuti, D. I., Firmansyah, Y. and Sugai, Y. (2024) Production, characterization, and application of *Pseudoxanthomonas taiwanensis* biosurfactant: a green chemical for microbial enhanced oil recovery (MEOR). *Science Reports,* **14(1)**, 10270. doi: 10.1038/s41598-024-61096-1.

4. Liu, J. F., Mbadinga, S. M., Yang, S. Z., Gu, J. D. and Mu, B. Z. (2015) Chemical structure, property, and potential applications of biosurfactants produced by Bacillus subtilis in petroleum recovery and spill mitigation. *International Journal of Molecular Sciences*, **16(3)**, 4814–4837.

5. Jezierska, S., Claus, S. and Van Bogaert, I. (2018) Yeast glycolipid biosurfactants. *FEBS Lett.*, **592(8)**, 1312–1329.

6. Liepins, J., Balina, K., Soloha, R., Berzina, I., Lukasa, L. K. and Dace, E. (2021) Glycolipid Biosurfactant Production from Waste Cooking Oils by Yeast: Review of Substrates, Producers and Products. *Fermentation*, **73,** 136.

7. Adetunji, A. I. and Olaniran, A. (2021) Production and potential biotechnological applications of microbial surfactants: An overview. *Saudi J. Biol. Sci.*, **28(1)**, 669–679.

8. Bratovcic, A., Nazdrajic, S., Odobasic, A. and Sestan, I. (2018) The influence of type of surfactant on physicochemical properties of liquid soap. *Int. J. Mater. Chem.*, **8**, 31-37.

9. Leonie, A. S., Maria da Gloria, C. S., Italo, J. B. D., Káren, G. O. B., Beatriz, G. R., Ivison, A. S., Matthew, S. T. and Ibrahim, M. B. (2022) Biosurfactants: Production, properties, applications, trends, and general perspectives. *Biochemical Engineering Journal*, **181**, 108377.

10. Yang, L., Guangze, Y., Yilun, W., Letao, X., Fei, H., Shankar, D., Chun-Xia, Z. (2023) Exploring biosurfactants as a sustainable alternative to chemical surfactants. *Colloids and Surfaces A: Physicochemical and Engineering Aspects.* **677**, Part A, 132291.

11. Wilson, R. J., Li, Y., Yang, G. and Zhao, C. -X. (2022) Nanoemulsions for drug delivery. *Particuology*, **85**, 97.

12. Wei, X., Ping, Y. and Alikhani, M. A. (2021) A Review on Biosurfactant Applications in the Petroleum Industry. *International Journal of Chemical Engineering*, **2021(1)**, 477185.

13. Md, F. (2012) Biosurfactant: Production and application. *Journal of Petroleum & Environmental Biotechnology*, **103(04)**, 1–6.

14. Mohan, P. K., Nakhla, G. and Yanful, E. K. (2006) Biokinetics of biodegradation of surfactants under aerobic, anoxic and anaerobic conditions. *Water Research,* **40(3)**, 533–540.

15. Desai, J. D. and Banat, I. M. (1997) Microbial production of surfactant and their commercial potential. *Microbiology and Molecular Biology Reviews*, **61(1)**, 47–64.

16. Kosaric, N. (2001) Biosurfactants and their application for soil bioremediation. *Food Technology and Biotechnology*, **39(4)**, 295–304.

17. Muthusamy, K., Gopalakrishnan, S., Ravi, T. K. and Sivachidambaram, P. (2008) Biosurfactants: properties, commercial production, and application. *Current Science*, **94(6)**, 736–774.

18. Chen, W., Kong, Y., Li, J., Sun, Y., Min, J. and Hu, X. (2020) Enhanced biodegradation of crude oil by constructed bacterial consortium comprising salt-tolerant petroleum degraders and biosurfactant producers. *International Biodeterioration and Biodegradation*, **154**, 105047.

19. Al-Bahry, S. N., Al-Wahaibi, Y. M., Elshafie, A. E., Al-Bemani, A. S., Joshi, S. J., Al-Makhmari, H. S. and Al-Sulaimani, H. S. (2013) Biosurfactant production by *Bacillus subtilis* B20 using date molasses and its possible application in enhanced oil recovery. *International Biodeterioration and Biodegradation*, **81**, 141–146.

20. Patowary, R., Patowary, K., Kalita, M. C. and Deka, S. (2018) Application of biosurfactant for enhancement of bioremediation process of crude oil contaminated soil. *International Biodeterioration and Biodegradation,* **129**, 50-60.

21. Liu, Q., Niu, J., Yu, Y., Wang, C., Lu, S., Zhang, S. and Peng, B. (2021) Production, characterization, and application of biosurfactant produced by Bacillus licheniformis L20 for microbial enhanced oil recovery. *Journal of Cleaner Production*, **307**, 127193.

22. Gogoi, D., Bhagowati, P., Gogoi, P., Bordoloi, N. K., Rafay, A., Dolui, S. K. and Mukherjee, A. K. (2016) Structural and physico-chemical characterization of a dirhamnolipid biosurfactant purified from: *Pseudomonas aeruginosa*:

Application of crude biosurfactant in enhanced oil recovery. *RSC Advances*, **6(74)**, 70669–70681.

23. Fariq, A. and Yasmin, A. (2020) Production, characterization, and bioactivities of biosurfactants from newly isolated strictly halophilic bacteria. *Process Biochemistry*, **98**, 1–10.

24. Him, N. R. N., Zainuddin, M. F. and Basha, A. Z. A. (2017) Fast biodegradation of toxic bisphenol a by Pseudomonas aeruginosa NR.22 (Ps.NR.22) isolated from Malaysian local lake. *AIP Conference Proceedings,* **1901(22)**, 100019.

25. Niku-Paavola, M. L., Raaska, L. and Itävaara, M. (1990) Detection of white-rot fungi by a non-toxic stain. *Mycological Research,* **94(1)**, 27–31.

26. Nik Raikhan, N. H. and Khairul Izwan, A. R. (2017) Novel treatment of heavily oiled wastewater using Pseudomonas aeruginosa Nr.22 producing usable free fatty acids (FFA). *International Journal of Conservation Science*, **8(3)**, 537–544.

27. Nik Him, N. R., Othman, N. H. and Zainuddin, M. F. (2017) Non-mediator supported novel natural oxidative biodegradation of Bisphenol A (BPA) in contaminated industrial wastewater by Pseudomonas aeruginosa NR. 22. *International Journal of Conservation Science*, **8(4)**, 685–694.

28. Vu, K. A., Tawfiq, K. and Chen, G. (2015) Rhamnolipid Transport in Biochar-Amended Agricultural Soil. *Water, Air, and Soil Pollution*, **226(8)**, 1–8.

29. Zhang, Y., Maier, W. J. and Miller, R. M. (1997) Effect of rhamnolipids on the dissolution, bioavailability, and biodegradation of phenanthrene. *Environmental Science and Technology*, **31(8)**, 2211–2217.

30. Burstone, M. S. (1956) A method of freeze-drying and its use in histochemistry and pathology. *Journal of the National Cancer Institute*, **17(1)**, 49–63.

31. Ghojavand, H., Vahabzadeh, F., Mehranian, M., Radmehr, M., Shahraki, K. A., Zolfagharian, F. and Roayaei, E. (2008) Isolation of thermotolerant, halotolerant, facultative biosurfactant- producing bacteria. *Applied Microbiology and Biotechnology*, **80(6)**, 1073–1085.

32. Nitschke, M. and Pastore, G. M. (2006) Production and properties of a surfactant obtained from Bacillus subtilis grown on cassava wastewater. *Bioresource Technology*, **97(2)**, 336–341.

33. Daverey, A. and Pakshirajan, K. (2010) Sophorolipids from Candida bombicola using mixed hydrophilic substrates: Production, purification, and characterization. *Colloids and Surfaces B: Biointerfaces*, **79(1)**, 246–253.

34. Cooper, D. G. and Goldenberg, B. G. (1987) Surface-active agents from two Bacillus species. *Applied and Environmental Microbiology*, **53(2)**, 224–229.

35. Pornsunthorntawee, O., Arttaweeporn, N., Paisanjit, S., Somboonthanate, P., Abe, M., Rujiravanit, R. and Chavadej, S. (2008) Isolation and comparison of biosurfactants produced by *Bacillus subtilis* PT2 and *Pseudomonas aeruginosa* SP4 for microbial surfactant-enhanced oil recovery. *Biochemical Engineering Journal*, **42(2)**, 172–179.

36. Syuhadah, B. H. and Nik Raikhan, N. H. (2022) Pseudomonas aeruginosa NR.22 – local hydrocarbon degrader species originated from crude oil non-exploration site: isolation, survivability and hydrocarbon degradation study. *Desalination and Water Treatment*, **257(22)**, 260–269.

37. Mojarad, M., Alemzadeh, A., Ghoreishi, G. and Javaheri, M. (2016) Kerosene biodegradation ability and characterization of bacteria isolated from oil-polluted soil and water. *Journal of Environmental Chemical Engineering*, **4(4)**, 4323-4329.

38. El-Sheshtawy, H. S., Aiad, I., Osman, M. E., Abo-ELnasr, A. A. and Kobisy, A. S. (2015). Production of biosurfactant from Bacillus licheniformis for microbial enhanced oil recovery and inhibition the growth of sulfate reducing bacteria. *Egyptian Journal of Petroleum,* **24(2),** 155–162.

39. Rodrigues, L. R., Teixeira, J. A., van der Mei, H. C. and Oliveira, R. (2006) Physicochemical and functional characterization of a biosurfactant produced by Lactococcus lactis 53. *Colloids and Surfaces B: Biointerfaces*, **49(1)**, 79–86.

40. Wei, Y. H., Chou, C. L. and Chang, J. S. (2005) Rhamnolipid production by indigenous Pseudomonas aeruginosa J4 originating from petrochemical wastewater. *Biochemical Engineering Journal*, **27(2)**, 146–154.

41. Dobler, L., De Carvalho, B. R., De Sousa Alves, W., Neves, B. C., Freire, D. M. G. and Almeida, R. V. (2017) Enhanced rhamnolipid production by Pseudomonas aeruginosa overexpressing estA in a simple medium. *PLoS ONE*, **12(8)**, 1–12.

42. Zhao, F., Shi, R., Ma, F., Han, S. and Zhang, Y. (2018) Oxygen effects on rhamnolipids production

by Pseudomonas aeruginosa. *Microbial Cell Factories*, **17(1)**, 1–11.

43. Kiefer, J., Radzuan, M. N. and Winterburn, J. (2017) Infrared spectroscopy for studying structure and aging effects in rhamnolipid biosurfactants. *Applied Sciences (Switzerland)*, **7(5)**.

44. Ghadir, S. El-H, Khaled. M. A., Mohammad. M. A. and Nadia, A. H. (2020) Structural and Physicochemical Characterization of Rhamnolipids produced by *Pseudomonas aeruginosa* P6. *AMB Express*, **10**, 201.

45. Eraqi, W. A., Yassin, A. S., Ali, A. E. and Amin, M. A. (2016) Utilization of Crude Glycerol as a Substrate for the Production of Rhamnolipid by *Pseudomonas aeruginosa*. *Biotechnology Research International*, **2016**, 1–9.

46. Sharma, D., Saharan, B. S., Chauhan, N., Bansal, A. and Procha, S. (2014) Production and structural characterization of *Lactobacillus helveticus* derived biosurfactant. *Scientific World Journal*, **2014**, 25–31.

47. Choe, B. -Y, Krishna, N. R. and Pritchard, D. G. (1992) Proton NMR study on rhamnolipids produced by Pseudomonas aeruginosa. *Magnetic Resonance in Chemistry*, **30(10)**, 1025–1026.

48. Lotfabad, T. B., Abassi, H., Ahmadkhaniha, R., Roostaazad, R., Masoomi, F., Zahiri, H. S. and Noghabi, K. A. (2010) Structural characterization of a rhamnolipid-type biosurfactant produced by Pseudomonas aeruginosa MR01: Enhancement of di-rhamnolipid proportion using gamma irradiation. *Colloids and Surfaces B: Biointerfaces*, **81(2)**, 397–405.

49. Mulligan, C. N. (2005) Environmental applications for biosurfactants. *Environmental Pollution*, **133(2)**, 183–198.

50. Matsufuji, M., Nakata, K. and Yoshimoto, A. (1997) High production of rhamnolipids by Pseudomonas aeruginosa growing on ethanol. *Biotechnology Letters*, **19(12)**, 1213–1215.

51. Hošková, M., Ježdík, R., Schreiberová, O., Chudoba, J., Šír, M., Čejková, A. and Řezanka, T. (2015) Structural and physiochemical characterization of rhamnolipids produced by Acinetobacter calcoaceticus, Enterobacter asburiae and Pseudomonas aeruginosa in single strain and mixed cultures. *Journal of Biotechnology*, **193**, 45–51.

52. Paulino, B. N., Pessôa, M. G., Mano, M. C. R., Molina, G., Neri-Numa, I. A. and Pastore, G. M. (2016) Current status in biotechnological production and applications of glycolipid biosurfactants. *Applied Microbiology and Biotechnology*, **100(24)**, 10265–10293.

53. Nitschke, M., Costa, S. G. V. A. O. and Contiero, J. (2005) Rhamnolipid surfactants: An update on the general aspects of these remarkable biomolecules. *Biotechnology Progress*, **21(6)**, 1593–1600.

54. Shreve, G. S. & Makula, R. (2019) Characterization of a new rhamnolipid biosurfactant complex from pseudomonas isolate DYNA270. *Biomolecules*, **9(12)**, 1–11.

55. Zhao, F., Shi, R., Zhao, J., Li, G., Bai, X., Han, S. and Zhang, Y. (2015) Heterologous production of Pseudomonas aeruginosa rhamnolipid under anaerobic conditions for microbial enhanced oil recovery. *Journal of Applied Microbiology*, **118(2)**, 379–389.

56. Lan, G., Fan, Q., Liu, Y., Chen, C., Li, G., Liu, Y. and Yin, X. (2015) Rhamnolipid production from waste cooking oil using Pseudomonas SWP-4. *Biochemical Engineering Journal*, **101**, 44–54.

57. Chen, C., Sun, N., Li, D., Long, S., Tang, X., Xiao, G. and Wang, L. (2018) Optimization and characterization of biosurfactant production from kitchen waste oil using Pseudomonas aeruginosa. *Environmental Science and Pollution Research*, **25(15)**, 14934–14943.

58. Sahebnazar, Z., Mowla, D., Karimi, G. & Yazdian, F. (2018) Zero-valent iron nanoparticles assisted purification of rhamnolipid for oil recovery improvement from oily sludge. *Journal of Environmental Chemical Engineering*, **6(1)**, 917–922.

59. Zhuo, W., Jim, J. W., Yili, M. J., Li, L. A., Gaston, L. M., Fultz, R. D. DeLaune (2020) Potential use of biochar and rhamnolipid biosurfactant for remediation of crude oil-contaminated coastal wetland soil: Ecotoxicity assessment. *Chemosphere*, **253**, 126617.

60. Lívia, V. A. de Castilho, Alan, M. D., Ilson, P. P., Joab, S. de Sousa, Fábio, C. S. N., José, G. C. G., Lucy, S., Denise, M. G. F. (2025) Mono- and di-rhamnolipids mixtures from Pseudomonas aeruginosa for use in extreme conditions of pre- and post-salt oil reservoirs compared with synthetic surfactants. *Colloids Surf B Biointerfaces*, **245**, 114311.

61. Singh, A. and Van Hamme, J. (2022) Bio-surfactants in petroleum recovery: Advances and environmental impact. *Bioresource Technology Reports*, **19**, 101204.

62. Ariech, M, Guechi, A. (2015) Assessment of four different methods for selecting biosurfactant producing extremely halophilic bacteria. *African Journal of Biotechnology*, **14(21)**, 1764–1772.

63. Isty, A. P., Maghfirotul, A., Dea, I. A., Yoga, F. and Yuichi, S. (2024) Production, characterization, and application of *Pseudoxanthomonas taiwanensis* biosurfactant: a green chemical for microbial enhanced oil recovery (MEOR). *Scientific Reports*, **14**, 10270.

64. Dobler, L., Ferraz, H. C., Araujo de Castilho, L. V., Sangenito, L. S., Pasqualino, I. P., Souza Dos Santos, A. L., Neves, B. C., Oliveira, R. R., Guimarães F. D. M. and Almeida, R. V. (2020) Environmentally friendly rhamnolipid production for petroleum remediation. *Chemosphere*, **252**, 126349. DOI: 10.1016/j. chemosphere. 2020.126349.

65. Kong, S., Shen, C., Li, Y. & Meng, Q. (2021) Rhamnolipids Sustain Unchanged Surface Activities during Decomposition in Alkaline Solutions. *ACS Omega*, **6(24)**, 15750–15755. DOI: 10.1021/acsomega.1c01099 PubMed.

66. Abdel-Mawgoud, A. M., Lépine, F. and Déziel, E. (2010) Rhamnolipids: diversity of structures, microbial origins, and roles. *Applied Microbiology Biotechnology*, **86**, 1323–1336.

67. Rosen Milton, J. & Kunjappu Joy, T. (2012) Surfactants and Interfacial Phenomena (4th Ed.). *Wiley*. ISBN: 978-0-470-54194-4 / 978-1-118-22893-7 qa.store.wiley.com+1.

68. Thakur, P., Saini, N. K., Thakur, V. K., Gupta, V. K., Saini, R. V. & Saini, A. K. (2021) *Rhamnolipid the Glycolipid Biosurfactant: Emerging trends and promising strategies in the field of biotechnology and biomedicine.* Microbial Cell Factories, **20**, 1. https://doi.org/10.1186/s12934-020-01497-9.

69. Li, Q. and Chong, H. (2017) Microbial production of rhamnolipids: opportunities, challenges, and strategies. *Microbial Cell Factories*, **16**, 137. DOI: 10.1186/s12934-017-0753-2.

70. Lavanya, M. (2024) Rhamnolipids: an insight to the overall characteristics of these extraordinary biomolecules. *Green Chemistry Letters and Reviews*, **17(1)**. https://doi.org/10.1080/17518253.2024.2371012

71. Dobler, L., Vilela, L. F., Almeida, R. V. & Freire, D. M. G. (2020) Rhamnolipids in perspective: Production, functional properties, and application in oil spill remediation. *Marine Pollution Bulletin*, **150**, 110685. https://doi.org/10.1016/j.marpolbul.2019.110685.

72. Kong, S., Zhu, X., Zhang, X. & Xu, H. (2021) Surface-active properties and emulsification performance of microbial rhamnolipids under different environmental conditions. *ACS Omega*, **6(30)**, 19434–19443. https://doi.org/10.1021/acsomega.1c02105.

73. Shrestha, R. G., Saha, B., Okajima, T. & Ohsaka, T. (2010) Interfacial tension reduction by sodium dodecyl sulfate and dioctyl sodium sulfosuccinate: Dynamic vs equilibrium behavior. *Journal of Colloid and Interface Science*, **348(2)**, 498–504. https://doi.org/10.1016/j.jcis.2010.04.054.

74. Rosen, M. J. & Kunjappu, J. T. (2012) Surfactants and interfacial phenomena (4th ed.). *Hoboken, NJ: Wiley*.

75. Thakur, P., Saini, H. S. & Singh, N. (2020) Rhamnolipids: The glycolipid biosurfactant—Emerging trends and promising applications. *Applied Microbiology and Biotechnology*, **104**, 9267–9292. https://doi.org/10.1007/s00253-020-10956-3.

76. Li, G., Zhang, Y., Wu, Q. & Zhu, L. (2017) Comparative biodegradation, and environmental behavior of biosurfactants and synthetic surfactants. *RSC Advances*, **7(80)**, 50563–50570. https://doi.org/10.1039/C7RA08757H.

77. David, A. R., Alon, V. (2014) The role of dispersants' dynamic interfacial tension in effective crude oil spill dispersion. *Marine Pollution Bulletin*, **84**, 155–163.